INTERNATIONAL JOURNAL FOR NUMERICAL METHODS IN FLUIDS, VOL. 21, 311–321 (1995)

A HIGHER-ORDER BOUNDARY ELEMENT METHOD FOR THREE-DIMENSIONAL POTENTIAL PROBLEMS

ZANG YUELONG

Engineering Mechanics Department, Xian Jiaotong University, Xian, China

AND

CHENG YUMIN AND ZHANG WU

Institute for Scientific Computing, Xian Jiaotong University, Xian, China

SUMMARY

A method of eliminating the singularities involved in boundary element methods for three-dimensional potential problems is presented and the non-singular expressions of integrals on an element on which the singular point is situated are given for linear and quadratic interpolation functions. Numerical examples are compared with analytical solutions to show that the higher-order interpolations have better precision.

KEY WORDS: high-order boundary element method; potential problems

1. INTRODUCTION

Boundary element methods (BEMs) are widely used in numerical calculations of engineering problems. In BEMs for various problems, proper fundamental solutions are needed and they usually have singularities which are involved in the integrations. It is well known that the boundary element method is a numerical method for solving boundary integral equations and the numerical procedure consists mainly of numerical integration to form a set of linear simultaneous equations of unknown values of nodal points on the boundary. After discretization the surface of the domain of the problem is divided into elements over which linear or quadratic interpolation functions are applied. The numerical integration can be carried out with Gauss quadrature if the singular point is not situated on the element and good accuracy can be obtained with an adequate number of Gauss integration points. However, when the singular point is on the element, the accuracy of numerical integration is greatly affected by it and an increase in the number of Gauss integration points is of no help owing to the singular behaviour of the integrand near the singular point.

For the singularities in boundary element methods of elasticity, Lachat[1] proposed a method of mapping the triangular element into a quadrilaterial to reduce one order of singularity and using rigid body motion to get rid of the influence of the remaining singularity. Rizzo and Shippy[2] used polar co-ordinates combined with rigid body motion prior to representing the displacement in terms of shape functions to treat singularities in elasticity. However, in potential problems there is no such special solution as rigid body motion in elasticity. Polar co-ordinates or degenerated mapping can only reduce one order of singularity in boundary element methods for potential problems. Cao *et al.*[3] have been successful in moving the singular points away from the boundary and outside the problem domain.

CCC 0271–2091/95/040311–11

Received May 1994
Revised January 1995

However, the desingularization distance in their method must be determined carefully according to the mesh size so that problems with uniqueness and ill-conditioning can be avoided.

Higher-order interpolation functions in boundary element methods are more and more used in practical numerical calculations owing to the higher accuracy and overall computational efficiency, including computer storage and CPU time required.[4,5] However, for different interpolation functions the singularity due to the fundamental solution is expressed in different ways and different methods have to be used to eliminate the singularity. In this paper it is shown that the singularity in the boundary elements for three-dimensional potential problems can be completely eliminated and for the linear element analytical expressions are given for the integral on the element on which the singular point is situated. Integral expressions devoid of singularity are also given for the quadratic element and the integral can be evaluated directly by Gauss quadrature.

2. BOUNDARY INTEGRAL EQUATION FOR POTENTIAL PROBLEMS

For a potential function ψ which satisfies the Laplace equation, we have the boundary integral equation[6]

$$\alpha(p)\psi(p) + \int_S \frac{\partial G(p,q)}{\partial n_q}\psi(q)\, dS_q = \int_S G(p,q)\frac{\partial \psi(q)}{\partial n_q}\, dS_q, \tag{1}$$

where p and q refer to the source point and field point respectively, $G(p, q)$ is the Green function or fundamental solution, S is the boundary surface of the domain of the problem, $\partial/\partial n_q$ refers to the normal derivative and $\alpha(p)$ is the solid angle at point p. Usually $G(p, q)$ is composed of a Rankine source, which is the inverse of the distance between the source point and the field point, and other non-singular terms:

$$G(p,q) = \frac{1}{r} + H(p,q) = \frac{1}{|r_p - r_q|} + H(p,q). \tag{2}$$

The non-singular term $H(p, q)$ makes no contribution to the solid angle $\alpha(p)$, *which* is determined solely by the first term (Rankine source) of (2) and the geometry at point p: $\alpha(p) = 4\pi$ when p is situated in the domain, $\alpha(p) = 2\pi$ when p is situated on a boundary which is smooth at point p, and $\alpha(p) = 0$ when p is outside the domain.

3. BOUNDARY ELEMENT INTERPOLATIONS

To solve the boundary integral equation (1) numerically, the boundary surface is discretized into a set of elements. Within each element, interpolation functions are adopted so that a certain number of nodal points on the element are representative of the element. The constant, linear and quadratic elements are mostly used in engineering computations. Here we consider the linear and quadratic ones. The interpolations for the co-ordinates and for the potential itself are

$$(x, y, z, \psi) = \sum_{k=1}^{n} N_k(\xi, \eta)(x_k, y_k, z_k, \psi_k), \tag{3}$$

where x_k, y_k, z_k and ψ_k are the nodal co-ordinates and potential values respectively and the shape functions $N_k(\xi, \eta)$ are

$$\begin{aligned} N_1 &= \tfrac{1}{4}(1+\xi)(1+\eta), & N_2 &= \tfrac{1}{4}(1-\xi)(1+\eta), \\ N_3 &= \tfrac{1}{4}(1-\xi)(1-\eta), & N_4 &= \tfrac{1}{4}(1+\xi)(1-\eta), \end{aligned} \tag{4}$$

for linear elements ($n=4$), and

$$\begin{aligned} N_1 &= \tfrac{1}{4}(1+\xi)(1+\eta)(\xi+\eta-1), & N_5 &= \tfrac{1}{2}(1-\xi^2)(1+\eta), \\ N_2 &= \tfrac{1}{4}(1-\xi)(1+\eta)(-\xi+\eta-1), & N_6 &= \tfrac{1}{2}(1-\eta^2)(1-\xi), \\ N_3 &= \tfrac{1}{4}(1-\xi)(1-\eta)(-\xi-\eta-1), & N_7 &= \tfrac{1}{2}(1-\xi^2)(1-\eta), \\ N_4 &= \tfrac{1}{4}(1+\xi)(1-\eta)(\xi-\eta-1), & N_8 &= \tfrac{1}{2}(1-\eta^2)(1+\xi), \end{aligned} \tag{5}$$

for quadratic elements ($n=8$), with $-1 \leqslant \xi, \eta \leqslant 1$.

4. TREATMENT OF SINGULARITY FOR LINEAR ELEMENT

From (2) we can see that when the field point q approaches the source point p, G(p, q) has a singularity. For the non-singular term $H(p, q)$, direct Gauss quadrature can be used without loss of accuracy. Here we concentrate on the Rankine source in (2). For an element on which the source point p is situated, it is supposed without loss of generality that point p is the nodal point 1 (see Figure 1). The singular integrals in (1) on the element are to be evaluated.

By means of Lachat's subelement we divide the element into two triangular elements (Figure 2) and map the subelement into a quadrilateral. On the quadrilateral element (see Figure 1(c)), interpolation functions (4) are used and the corresponding Jacobian can be expressed as

$$J(\xi,\eta) = \frac{1-\eta}{16}\sqrt{(b_1^2+b_2^2+b_3^2)}, \tag{6}$$

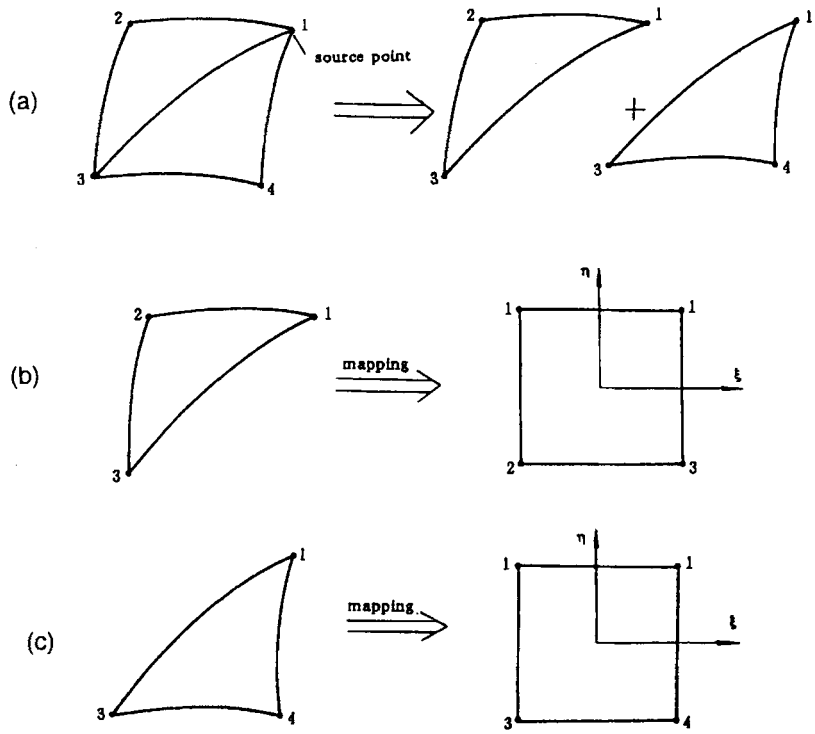

Figure 1. Subdivision of an element and degenerate mapping. (a) Subdivision of a four-node linear element into two triangular subelements. (b) Mapping of the first subelement into a quadrilateral. (c) Mapping of the second subelement into a quadrilateral

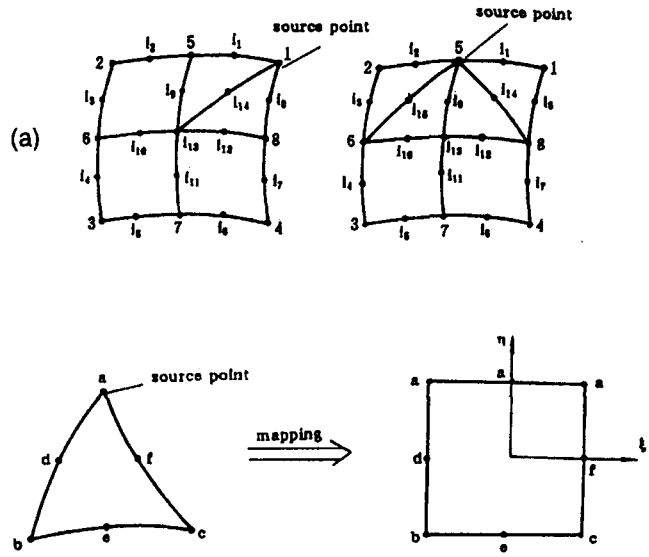

Figure 2. Subdivision of a quadratic element and degenerate mapping. (a) Subdivision and interposition of temporary interpolation points $i_1, i_2, \ldots, i_{15}$ when the source point is node 1 or node 5. (b) Mapping of a six-node triangular element into a quadrilateral with node a as the source point

where

$$b_1 = (y_4 - y_3)(2z_1 - z_3 - z_4) - (z_4 - z_3)(2y_1 - y_3 - y_4),$$

$$b_2 = (z_4 - z_3)(2x_1 - x_3 - x_4) - (x_4 - x_3)(2z_1 - z_3 - z_4),$$

$$b_3 = (x_4 - x_3)(2y_1 - y_3 - y_4) - (y_4 - y_3)(2x_1 - x_3 - x_4).$$

There is a degeneracy in the map when η approaches unity, which means that the field point approaches the source point. The degeneracy obviously reduces one order of singularity. The unit normal vector of the element is expressed as

$$n = \frac{b_1 i + b_2 j + b_3 k}{\sqrt{(b_1^2 + b_2^2 + b_3^2)}}, \tag{7}$$

where **i**, **j** and **k** are unit vectors along the co-ordinate axes. The distance between p and q is

$$r = (1 - \eta)\sqrt{[a_1^2(\xi) + a_2^2(\xi) + a_3^2(\xi)]}, \tag{8}$$

where

$$a_1(\xi) = \tfrac{1}{4}(1 - \xi)x_3 + \tfrac{1}{4}(1 + \xi)x_4 - \tfrac{1}{2}x_1.$$

The terms $a_2(\xi)$ and $a_3(\xi)$ can be obtained by replacing x with y and z respectively without changing the subscripts involved. Because $a_1(\xi)\ b_1 + a_2(\xi); b_2 + a_3(\xi)b_3 = 0$, which can be easily proved directly from the orthogonal relationship between the normal vector **n** of the plane element and the vector **r** pointing from the source point to the field point, the normal derivative

of $G(p, q)$ on the element becomes

$$\frac{\partial G(p,q)}{\partial n} = -\frac{(x-x_1)n_1+(y-y_1)n_2+(z-z_1)n_3}{r^3}+\frac{\partial H(p,q)}{\partial n}$$
$$= -\frac{a_1(\xi)b_1+a_2(\xi)b_2+a_3(\xi)b_3}{\sqrt{(b_1^2+b_2^2+b_3^2)}[a_1^2(\xi)+a_2^2(\xi)+a_3^2(\xi)]^{3/2}(1-\eta)^2}+\frac{\partial H(p,q)}{\partial n}$$
$$= \frac{\partial H(p,q)}{\partial n}. \tag{9}$$

The first integral in (1) on the subelement is written as

$$\int_{S_e}\frac{\partial G(p,q)}{\partial n_q}\psi(q)\,dS_q = \frac{\sqrt{(b_1^2+b_2^2+b_3^2)}}{16}\sum_{k=1}^{4}\psi_k\int_{-1}^{1}\int_{-1}^{1}\frac{\partial H(p,q)}{\partial n_q}(1-\eta)N_k(\xi,\eta)\,d\xi\,d\eta, \tag{10}$$

where $k=1$, 2, 3 and 4 correspond to nodes 1, 1, 2 and 3 respectively for the first subelement and to nodes 1, 1, 3 and 4 respectively for the second subelement. As for the second integral in (1), if $\partial\psi/\partial n$ is also interpolated as the co-ordinates in (3), considering (6) and (8), we have

$$\int_{S_e}G(p,q)\frac{\partial\psi(q)}{\partial n_q}\,dS_q = \frac{\sqrt{(b_1^2+b_2^2+b_3^2)}}{16}\sum_{k=1}^{4}\left(\frac{\partial\psi}{\partial n}\right)_k\int_{-1}^{1}\int_{-1}^{1}$$
$$\times\left(\frac{1}{\sqrt{[a_1^2(\xi)+a_2^2(\xi)+a_3^2(\xi)]}}+(1-\eta)H(p,q)\right)N_k(\xi,\eta)\,d\xi\,d\eta. \tag{11}$$

Obviously the right-hand-side integrals in (10) and (11) and normal double integrals and Gauss quadrature can be used directly. The first term in the large parentheses multiplied by $N_k(\xi,\eta)$ in the integrand of (11) can be integrated analytically and (11) can be written as

$$\int_{S_e}G(p,q)\frac{\partial\psi(q)}{\partial n_q}\,dS_q = \frac{\sqrt{(b_1^2+b_2^2+b_3^2)}}{16}$$
$$\times\sum_{k=1}^{4}\left(\frac{\partial\psi}{\partial n}\right)_k\left(2\lambda_k+\int_{-1}^{1}\int_{-1}^{1}H(p,q)(1-\eta)N_k(\xi,\eta)\,d\xi\,d\eta\right), \tag{12}$$

where $\lambda_1=\lambda_4=u+v$, $\lambda_2=\lambda_3=u-v$ and

$$u=\frac{1}{c_1}ln\left|\frac{\sqrt{(c_1+2c_2+c_3)}+\sqrt{c_1+c_2/\sqrt{c_1}}}{\sqrt{(c_1-2c_2+c_3)}-\sqrt{c_1+c_2/\sqrt{c_1}}}\right|,$$
$$v=\frac{1}{c_1}[\sqrt{(c_1+2c_2+c_3)}-\sqrt{(c_1-2c_2+c_3)}-c_2u],$$
$$c_1=(x_4-x_3)^2+(y_4-y_3)^2+(z_4-z_3)^2,$$
$$c_2=(x_4-x_3)(x_4+x_3-2x_1)+(y_4-y_3)(y_4+y_3-2y_1)+(z_4-z_3)(z_4+z_3-2z_1),$$
$$c_3=(x_4+x_3-2x_1)^2+(y_4+y_3-2y_1)^2+(z_4+z_3-2z_1)^2$$

for subelement Δ_{134}. The corresponding expressions for subelement Δ_{123} are obtained if subscripts 3 and 4 are replaced by 2 and 3 respectively.

5. TREATMENT OF SINGULARITY FOR QUADRATIC ELEMENT

The source point may be any one of the eight nodal points on a quadratic element. Lachat's subelement method is still used to divide the element into several subelements. There are two cases: the source

point can be one of the four corner points or one of the four side midpoints. There are several ways of subdividing the element. For some ways, certain temporary interpolation points have to be arranged so that the subelements are still quadratic ones. After integration the temporary interpolation points are condensed. Whatever the method of subdivision, the source point is always arranged on the vertices of some triangular subelements and degenerate mapping is used to reduce one-order of singularity. For a six-node triangular element (which is taken to be a degenerate quadrilateral with the degenerated side coinciding with the source point) (see Figure 2), if equations (5) are still used as shape functions, the Jacobian is

$$J(\xi,\eta)=\frac{1-\eta}{16}\sqrt{[B_1^2(\xi,\eta)+B_2^2(\xi,\eta)+B_3^2(\xi,\eta)]}, \tag{13}$$

where

$$\begin{aligned}B_1(\xi,\eta)=&\,2(1+2\eta)(2\xi+\eta)(y_bz_a-y_az_b)+2(1+2\eta)(2\xi-\eta)(y_cz_a-y_az_c)\\&+4(1+\eta)(1+2\eta)(y_az_d-y_dz_a)+8\xi(1+2\eta)(y_az_e-y_ez_a)\\&+4(1+\eta)(1+2\eta)(y_fz_a-y_az_f)+2(2\xi^2-2\eta^2-3\xi^2\eta)(y_cz_b-y_bz_c)\\&+2(1-\xi)(\xi+2\eta-3\xi\eta)(y_bz_d-y_dz_b)+2(1-\xi)(3\xi\eta-2\xi-\eta)(y_bz_e-y_ez_b)\\&+2(\xi-2\eta+3\xi\eta+\xi^2-4\eta^2-3\xi^2\eta)(y_dz_c-y_cz_d)+2(1+\xi)(2\xi-\eta-3\xi\eta)(y_ez_c-y_cz_e)\\&+2(1+\xi)(2\eta-\xi+3\xi\eta)(y_fz_c-y_cz_f)+4(1+\eta-4\xi\eta-\xi^2+3\xi^2\eta)(y_dz_e-y_ez_d)\\&+16\eta(1+\eta)(y_dz_f-y_fz_d)+4(1+\eta+4\xi\eta-\xi^2+3\xi^2\eta)(y_ez_f-y_fz_e)\\&+2(\xi+2\eta+3\xi\eta-\xi^2+4\eta^2+3\xi^2\eta)(y_fz_b-y_bz_f).\end{aligned}$$

$B_2(\xi,\eta)$ is obtained if y and z are replaced by z and x respectively and $B_3(\xi,\eta)$ is obtained by replacing y and z with x and y respectively. We can see that (13) is just like (6), but the terms in the square root are much more complicated. The distance between the source point and the field point can be expressed as

$$r=\frac{1-\eta}{4}\sqrt{[A_1^2(\xi,\eta)+A_2^2(\xi,\eta)+A_3^2(\xi,\eta)]}, \tag{14}$$

where

$$\begin{aligned}A_1(\xi,\eta)=&-2(2+\eta)x_a-(1-\xi)(\xi+\eta+1)x_b+(1+\xi)(\xi-\eta-1)x_c\\&+2(1+\eta)(1-\xi)x_d+2(1-\xi^2)x_e+2(1+\eta)(1+\xi)x_f.\end{aligned}$$

$A_2(\xi,\eta)$ and $A_3(\xi,\eta)$ are obtained if x is replaced by y and z respectively in the expression of $A_1(\xi,\eta)$. Through tedious deduction we obtain

$$\begin{aligned}\frac{\partial G}{\partial n}=&\frac{\partial H(p,q)}{\partial n}\\&-\frac{64\Pi_{abcdef}}{(1-\eta)[A_1^2(\xi,\eta)+A_2^2(\xi,gh)+A_3^2(\xi,\eta)]^{3/2}\sqrt{[B_1^2(\xi,\eta)+B_2^2(\xi,\eta)+B_3^2(\xi,\eta)]}},\end{aligned} \tag{15}$$

where

$$\begin{aligned}\Pi_{abcdef} =&(4\xi^2+\xi^2\eta+\eta)\Delta_{abc}+(1-\xi)(1-3\xi-\xi\eta)_{abd}+(1-\xi)(4\xi+\eta+\xi\eta)\Delta_{abe}\\&+(1+2\eta+\xi\eta+3\xi^2+\xi^2\eta)\Delta_{acd}+(1+\xi)(4\xi+\xi\eta-\eta)\Delta_{ace}\\&-(1+\xi)(1+3\xi+\xi\eta)\Delta_{acf}-2(1-\xi)(1+3\xi+\eta+\xi\eta)\Delta_{ade}+4(1+\eta)\Delta_{adf}\\&-2(1+\xi)(1-3\xi+\eta-\xi\eta)\Delta_{aef}-(1+2\eta-\xi\eta+3\xi^2+\xi^2\eta)\Delta_{abf}\\&+\xi(1-\xi)(1-\xi+\eta)\Delta_{bcd}-\eta(1-\xi^2)\Delta_{bce}-\xi(1+\xi)(1+\xi+\eta)\Delta_{bcf}\\&-(1-\xi)^3\Delta_{bde}+2\xi(1-\xi)(1+\eta)\Delta_{bdf}-(1-\xi^2)(1+\xi+2\eta)\Delta_{bef}\\&-(1-\xi^2)(1-\xi+2\eta)_{cde}-2\xi(1+\xi)(1+\eta)\Delta_{cdf}-(1+\xi)^3\Delta_{cef}\\&+4(1-\xi^2)(1+\eta)\Delta_{def},\end{aligned}$$

$$\Delta_{abc}=\begin{vmatrix}x_a & x_b & x_c\\ y_a & y_b & y_c\\ z_a & z_b & z_c\end{vmatrix},\quad\ldots,\quad\Delta_{def}=\begin{vmatrix}x_d & x_e & x_f\\ y_d & y_e & y_f\\ z_d & z_e & z_f\end{vmatrix}.$$

From (15) we can see that there is only one order of singularity which is represented by the inverse of $1-\eta$ which is going to be eliminated by the same factor in the expression of the Jacobian (13). The first integral in (1) on the subelement becomes

$$\int_{S_e}\frac{\partial G}{\partial n}\psi\,dS=\sum_{k=1}^{8}\psi_k\int_{-1}^{1}\int_{-1}^{1}\left(-\frac{4\Pi_{abcdef}}{[A_1^2(\xi,\eta)+A_2^2(\xi,\eta)+A_3^2(\xi,\eta)]^{3/2}}+\frac{1-\eta}{16}\sqrt{[B_1^2(\xi,\eta)+B_2^2(\xi,\eta)+B_3^2(\xi,\eta)]}\,\frac{\partial H(p,q)}{\partial n}\right)N_k(\xi,\eta)\,d\xi\,d\eta \tag{16}$$

and the second integral in (1) on the subelement is

$$\int_{S_e}G\frac{\partial\psi}{\partial n}dS=\frac{1}{4}\int_{-1}^{1}\int_{-1}^{1}\frac{\sqrt{[B_1^2(\xi,\eta)+B_2^2(\xi,\eta)+B_3^2(\xi,\eta)]}}{\sqrt{[A_1^2(\xi,\eta)+A_2^2(\xi,\eta)+A_3^2(\xi,\eta)]}}\frac{\partial\psi}{\partial n}\,d\xi\,d\eta+\int_{S_e}H(p,q)\frac{\partial\psi}{\partial n}\,dS \tag{17}$$

or

$$\begin{aligned}\int_{S_e}G\frac{\partial\psi}{\partial n}dS=&\frac{1}{4}\sum_{k=1}^{8}\left(\frac{\partial\psi}{\partial n}\right)_k\int_{-1}^{1}\int_{-1}^{1}\frac{\sqrt{[B_1^2(\xi,\eta)+B_2^2(\xi,\eta)+B_3^2(\xi,\eta)]}}{\sqrt{[A_1^2(\xi,\eta)+A_2^2(\xi,\eta)+A_3^2(\xi,\eta)]}}N_k(\xi,\eta)\,d\xi\,d\eta\\&+\sum_{k=1}^{8}\left(\frac{\partial\psi}{\partial n}\right)_k\int_{-1}^{1}\int_{-1}^{1}H(p,q)N_k(\xi,\eta)\,d\xi\,d\eta\end{aligned} \tag{17'}$$

if $\partial/\partial n$ is also interpolated with the shape functions (5). In (16) and (17) $k=1, 2,\ldots,8$ correspond to nodes a, a, b, c, a, d, e and f respectively (see Figure 2). Gauss quadrature is used directly for (16) and (17). For other subelements without the source point the integrals in (1) are non-singular and Gauss quadrature can be used with non-degenerate mapping.

6. NUMERICAL EXAMPLES

Two numerical examples are considered. The first is the potential field calculation of a sphere with radius a (in the numerical calculation a is taken to be unity) moving in an infinite body of water. The analytical solution to this problem is

$$\psi = \frac{Ua^3 x}{2(x^2+y^2+z^2)^{3/2}}, \tag{18}$$

where U is the velocity of the sphere, the origin of the co-ordinate system $Oxyz$ coincides with the centre of the sphere and the x-axis is taken to be parallel to the direction of movement of the sphere.

The corresponding boundary condition on the interface between the sphere and the water is

$$\frac{\partial \psi}{\partial n} = -Un_1. \tag{19}$$

Substituting (19) in (1) gives

$$\alpha(p)\psi(p) + \int_S \frac{\partial G(p,q)}{\partial n_q}\psi(q)\,dS_q = -U\int_S G(p,q)n_1(q)\,dS_q, \tag{20}$$

where S is the surface of the sphere and hence $\alpha(p) = 2\pi$. The Rankine source function can be taken as the fundamental solution.

In this case the integral on the subelement on which the field point and the source point coincide may be written according to the last two sections as

$$\int_{S_e} \frac{\partial G(p,q)}{\partial n_q}\psi(q)\,dS_q = 0,$$

$$\int_{S_e} G(p,q)n_1(q)\,dS_q = \tfrac{1}{2}b_1 u$$

for the linear element with interpolations equations (3) and (4) and as

$$\int_{S_e} \frac{\partial G(p,q)}{\partial n_q}\psi(q)\,dS_q = -4\sum_{k=1}^{8}\psi_k \int_{-1}^{1}\int_{-1}^{1} \frac{N_k \Pi_{abcdef}}{(A_1^2+A_2^2+A_3^2)^{3/2}}\,d\xi\,d\eta,$$

$$\int_{S_e} G(p,q)n_1(q)\,dS_q = \frac{1}{4}\int_{-1}^{1}\int_{-1}^{1} \frac{B_1}{\sqrt{(A_1^2+A_2^2+A_3^2)}}\,d\xi\,d\eta$$

for the quadratic element with interpolation equations (3) and (5).

In the numerical calculation we first discretize the surface of the sphere with 45 nodal points using quadratic elements (considering symmetry with respect to the y-axis) (see Figure 3) and 57 nodal points using linear elements. The latter mesh is obtained by adding nodal points at the centres of the quadratic elements in the former mesh. The piecewise constant element is also used to calculate the same problem and the corresponding mesh is the same as that for the linear element. For the piecewise constant element the geometry is still interpolated with linear interpolation functions.

Further, the mesh is refined with 161 nodal points for the quadratic element and with 209 nodal points for the linear element. The results are presented in Table I in comparison with the analytical

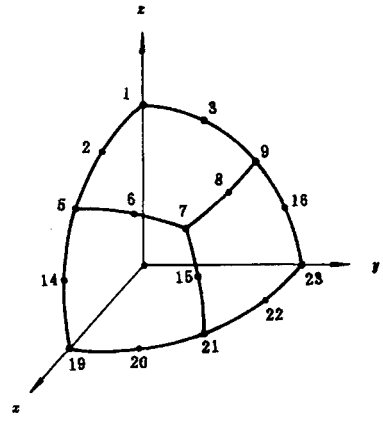

Figure 3. Quadratic element arrangement on a quadrant of a sphere surface

Table I. Potential values at given nodal points*

No.	LE, $N = 57$	QE, $N = 45$	LE, $N = 209$	QE, $N = 161$	Analytical
2	0·1855	0·1905	0·1899	0·1913	0·1913
5	0·3458	0·3500	0·3512	0·3534	0·3536
6	0·3292	0·3329	0·3347	0·3368	0·3369
7	0·2832	0·2856	0·2873	0·2885	0·2887
8	0·1503	0·1518	0·1513	0·1512	0·1515
14	0·4526	0·4566	0·4591	0·4617	0·4619
15	0·3292	0·3329	0·3352	0·3368	0·3369
19	0·4899	0·4950	0·4972	0·4998	0·5000
20	0·4526	0·4565	0·4597	0·4617	0·4619
21	0·3458	0·3500	0·3522	0·3534	0·3536
22	0·1855	0·1905	0·1909	0·1913	0·1913

* LE, linear element; QE, quadratic element; N, number of nodes.

solution (18). If the RMS error is considered, which is defined as

$$E_{rms} = \sqrt{\left(\frac{1}{N}\sum_{i=1}^{N}(\psi_{ana} - \psi_{num})^2\right)},$$

where N is the number of nodal points and ψ_{ana} and ψ_{num} are the analytical and numerical values respectively, we find that the quadratic interpolation gives better precision with fewer nodal points and that the linear interpolation is better than the piecewise constant approximation. Values of E_{rms} for different nodal points and different interpolations are given in Table II.

The second example is taken from Reference 3. It is a Dirichlet problem with a dipole of unit strength located at (0, 0, -1) and the dipole direction parallel to the x-axis. The normal derivative $\partial\psi/\partial n$ is sought on $z = 0$ on which the boundary condition $\psi = 0$ is imposed.

In this case appropriate source points are arranged on the boundary $z = 0$. The domain is the lower half-space below $z = 0$. We can isolate the singularity of the dipole by decomposing the potential ψ into regular and singular parts:

$$\psi = \bar{\psi} - \frac{1}{4\pi}\frac{1}{[x^2 + y^2 + (z+1)^2]^{3/2}}. \tag{21}$$

Table II. RMS errors for different interpolation functions

N	45	57	161	209
QE	0·003246	—	0·0002138	—
LE	—	0·006413	—	0·004056
Const.	—	0·011611	—	0·006627

Substituting (21) in (1) and considering that both the source point and the field point are on the same plane $z=0$ and hence the normal derivative of the Rankine source function is always zero, we have the integral equation

$$\int_{z=0} \frac{1}{|r_q - r_p|} \frac{\partial \bar{\psi}(q)}{\partial n_q} dS_q = \alpha(p)\bar{\psi}(p), \quad p, q \in z = 0.$$

Since $\psi = 0$ on $z=0$ and the surface $z=0$ is smooth everywhere, i.e. $\alpha(p)=2\pi$, we finally have

$$\int_{z=0} \frac{1}{|r_q - r_p|} \frac{\partial \bar{\psi}(q)}{\partial n_q} dS_q = \frac{1}{2} \frac{x_p}{(x_p^2 + y_p^2 + 1)^{3/2}}. \tag{22}$$

The discretization on $z=0$ must be carefully arranged for this case. On $z=0$ near the dipole the size of elements should not be over 0·6 for quadratic interpolation and 0·1 for linear interpolation, otherwise, even if the nodal points of an element have exact values, the interpolations cannot give good precision, and vice versa, if the interpolations do not have good precision, the final results of nodal points will not be satisfactory. The size of elements can be gradually increased as the discretized portion gets farther away from the dipole. Another factor which must be considered is the truncation of the surface $z=0$. However, owing to the rapid decay property, truncation the $z=0$ plane at $R_\infty = |x_{\max}| = |y_{\max}| = 5$ (symmetry with respect to y is considered) seems to be appropriate. In Table III the RMS errors are given in relation to the truncation distance R_∞ and the number of nodal points N for the quadratic element. Table IV gives the RMS errors for the linear interpolation and the piecewise constant approximation. It is obvious from Tables III and IV that the quadratic interpolation gives lower RMS errors with fewer nodal points than the linear interpolation, which in turn has lower RMS errors than the piecewise constant approximation with the same number of elements. (In the case of the piecewise constant approximation the source point is arranged at the centroids of the elements and hence with the same mesh as for the linear interpolation the piecewise approximation has fewer source points.)

Table III. E_{rms} for quadratic interpolation

N	121	181	253	337	443
R_∞	2·0	3·0	4·0	5·0	7·0
E_{rms}	0·0012084	0·0003383	0·0002116	0·0001709	0·0001458

Table IV. E_{rms} for piecewise constant approximation (C) and linear interpolation (L)

N	231	325	435	561	703
R_∞	2·0	3·0	4·0	5·0	7·0
E_{rms}(C)	0·002743	0·002141	0·001826	0·001596	0·001418
E_{rms}(L)	0·0009725	0·0004098	0·000317	0·000274	0·000242

7. CONCLUSIONS

A higher-order boundary element method for three-dimensional potential problems is presented. Integral expressions devoid of singularity are given for both linear and quadratic elements and Gauss quadrature can be used directly to evaluate the integrals numerically. Numerical examples are compared satisfactorily with analytical solutions. For the examples we find that the higher-order interpolation functions give higher accuracy, especially for problems with complicated geometry.

REFERENCES

1. J. C. Lachat, 'A further development of the boundary integral technique for elastostatics', *Dissertation*, University of Southampton, 1975.
2. F. J. Rizzo and D. J. Shippy, 'An advanced boundary integral equation method for the three-dimensional thermo-elasticity', *Int. j. numer. methods eng.*, **11**, 1753–1768 (1977).
3. Y. Cao, W. W. Schultz and R. F. Beck, 'Three-dimensional desingularized boundary integral methods for potential problems', *Int. j. numer. methods fluids*, **12**, 785–803 (1991).
4. C. R. Chan, A. N. Beris and S. G. Advani, 'Second order boundary element method calculations of hydrodynamic interactions between particles in close proximity', *Int. j. numer. methods fluids*, **14**, 1063–1086 (1992).
5. C. R. Chan, A. N. Beris and S. G. Advani, 'Analysis of periodic 3D viscous flows using a quadratic discrete Galerkin boundary element method', *Int. j. numer. methods fluids*, **18**, 953–981 (1994).
6. C. A. Brebbia, J. C. F. Telles and L. C. Wrobel, *Boundary Element Techniques—Theory and Applications in Engineering*, Springer, New York, 1984.